PHYSICAL REVIEW B **85**, 081402(R) (2012)

Trapping surface electrons on graphene layers and islands

D. Niesner,[1] Th. Fauster,[1] J. I. Dadap,[2] N. Zaki,[2] K. R. Knox,[2] P.-C. Yeh,[2] R. Bhandari,[2] R. M. Osgood,[2] M. Petrović,[3] and M. Kralj[3]

[1]*Lehrstuhl für Festkörperphysik, Universität Erlangen-Nürnberg, D-91058 Erlangen, Germany*

[2]*Columbia University, New York, New York 10027, USA*

[3]*Institut za fiziku, Bijenička 46, HR-10000 Zagreb, Croatia*

(Received 9 September 2011; revised manuscript received 26 January 2012; published 13 February 2012)

We report the use of time- and angle-resolved two-photon photoemission to map the bound, unoccupied electronic structure of the weakly coupled graphene/Ir(111) system. The energy, dispersion, and lifetime of the lowest three image-potential states are measured. In addition, the weak interaction between Ir and graphene permits observation of resonant transitions from an unquenched Shockley-type surface state of the Ir substrate to graphene/Ir image-potential states. The image-potential-state lifetimes are comparable to those of midgap clean metal surfaces. Evidence of localization of the excited electrons on single-atom-layer graphene islands is provided by coverage-dependent measurements.

DOI: 10.1103/PhysRevB.85.081402 PACS number(s): 73.22.Pr, 73.20.−r, 79.20.Ws, 79.60.Dp

Graphene on metal surfaces is a materials system of enormous fundamental and applied interest.[1] The graphene/metal interface is encountered in the rapidly expanding technological system of graphene on Cu foil produced by chemical vapor deposition (CVD),[2] in the structurally precise monolayer epitaxial systems of graphene on single-crystal Ir and Ru,[3,4] and finally in the metal contacts of graphene field-effect transistors[5] or other devices for transport measurements.[6] Questions then arise on the electronic structure of graphene on metal surfaces, and in fact several recent studies have addressed questions such as the role of lattice mismatch on band structures. Most studies of the electronic structure of graphene have focused on the band structure in the vicinity of its K point, near the Fermi edge.[7–9] Further, there has been a paucity of measurements about its unoccupied electronic structure and the dynamics of strongly excited electrons.[10] Image-potential states offer one important approach to probe the excited-state manifold and are known to vary with interfacial quality, dielectric properties, and electronic structure. In graphene the large band gap at the Γ point results in Bragg reflection from the crystal within a certain range of energy and momentum. In fact, a recent theoretical study has shown the existence of a dual Rydberg-like series of even and odd symmetry image-potential states in a single free-standing sheet of graphene.[11] Image-potential states on graphene may experience different dynamic constraints. For example, the different phase space for decay in two dimensions compared to three dimensions may affect the lifetimes for electrons trapped in image-potential states on graphene. In fact, more generally the response of the image-potential electron to the composite dielectric/metal systems is itself of basic physics interest.

In this Rapid Communication, we investigate the uncharted region of the bound, unoccupied electronic structure of epitaxial graphene grown on Ir(111) in the vicinity of the graphene Γ point; our measurements are made via the image-potential states using angle- and time-resolved two-photon photoemission (2PPE), as indicated by arrows in Fig. 1. This system was chosen for several reasons: First, because of the weak coupling in the graphene/Ir(111) system, the electronic structure of the graphene overlayer is nearly intact, with sharp Dirac dispersion characteristics.[12] In addition, the moiré corrugation of the epitaxial graphene on Ir(111) has been found to be only 0.35 ± 0.10 Å based on atomic force microscopy measurements,[13] indicating a smooth epitaxial graphene surface. Second, the molecular-based growth is well characterized and saturates at precisely one monolayer (ML) of epitaxial graphene.[14] Our results show that image-potential states may be excited from the Ir/graphene interfacial region and have binding energies and lifetimes comparable to those of midgap clean metal surfaces. In addition, spectral measurements of binding energy versus coverage show clearly that at low graphene coverage, image-potential electrons are trapped on graphene islands by surface work-function differences between the metal and graphene regions, an observation of high importance for understanding of transport at graphene-metal interfaces.[15]

Our choice of two-photon photoemission is the result of its high temporal and energy resolution. Other experimental observations of image-potential states have used scanning tunneling spectroscopy, i.e., graphene on SiC (Ref. 16) and on Ru(0001).[17] This technique, however, measures the image-potential series in the presence of a strongly distorting electric field between the tip and sample and without time-resolved possibilities.

The experiments were conducted using monochromatic and bichromatic 2PPE, and angle-resolved photoemission (ARPES). Details of the monochromatic 2PPE setup at Columbia University, which was used in the photon energy range of $3.8 < h\nu < 4.9$ eV, are given in Ref. 18. Bichromatic and time-resolved 2PPE measurements were performed in Erlangen using pump-probe methods with the third harmonic (UV) and the fundamental (IR, $1.51 < h\nu < 1.62$ eV) as described in Ref. 19. Additionally, occupied-state ARPES measurements were performed at APE (ELETTRA) using a photon energy of 55 eV with an energy resolution of 20 meV. The resolution of the 2PPE experiments was 40 meV. The base pressure in all three ultrahigh vacuum (UHV) systems was better than 1×10^{-8} Pa. All measurements used p-polarized beams.

Graphene was prepared by cycles of temperature programed growth (TPG) (room-temperature ethene exposure 6×10^{-6} Pa for 60 s and flashed to ≈1450 K), followed by

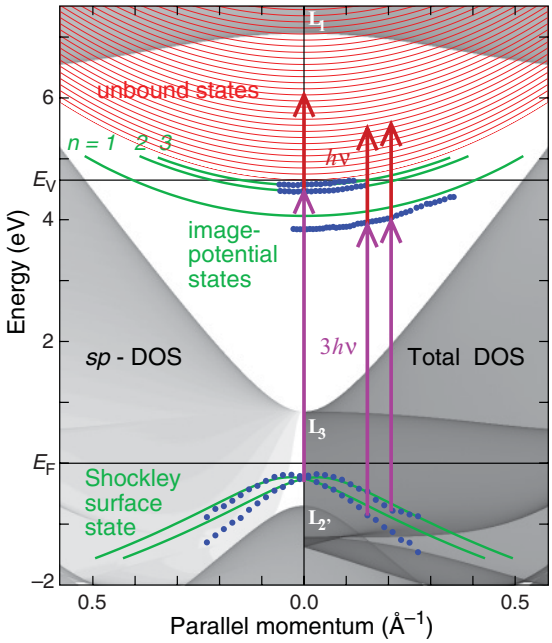

FIG. 1. (Color online) Arrows indicate 2PPE transitions between surface and image-potential states. The experimental results (dots) are compared to calculations (lines). The projected bulk-band structure of Ir(111) along the Γ*K* direction is shaded according to the total and *sp* density of states (DOS) at the right and left, respectively.

a chemical vapor deposition run (6×10^{-6} Pa of ethene for 300 s at 1150 K), to form exactly one graphene monolayer.[14] Growth was monitored by low-energy electron diffraction (LEED) after each cycle, which showed the development of the characteristic moiré pattern of uniformly oriented graphene,[20] as graphene coverage varied from 0 to 1 ML; LEED patterns (not shown) revealed these patterns clearly.

Figure 2(a) shows the measured 2PPE intensity obtained at 1 ML and for $h\nu = 1.59$ eV along the Γ*K* direction. Three unoccupied bands are observed. The pumping process could be deduced from its photon-energy dependence, thus in the bichromatic case, all peak positions shifted linearly with IR photon energy, indicating that the process involves pumping by a UV photon and photoemission by an IR photon.[21] All 2PPE features vanished when the IR beam was switched to *s* polarization, indicating the expected symmetry for image-potential states. The effective masses of all three states are $0.9 \pm 0.1 m_e$. The binding energies of the three states with respect to the vacuum level are given in Table I. The measured energies and effective masses are close to the free-electron mass and fit well to a Rydberg-like series of image-potential states with a nonvanishing quantum defect.[22]

TABLE I. Experimental and calculated binding energies and lifetimes for image-potential states on graphene/Ir(111).

n	E_n^{exp} (eV)	E_n^{calc} (eV)	τ (fs)
1	0.83 ± 0.02	0.59	35 ± 3
2	0.19 ± 0.02	0.18	114 ± 6
3	0.09 ± 0.02	0.08	270 ± 12

Figure 2(a) shows that the $n = 1$ band is most intense for parallel momenta $k_\parallel$ between 0.08 and 0.17 Å^{-1} [cf. points in Fig. 2(a)], with the intensity typically decreasing monotonically with increasing $k_\parallel$.[23] Direct transitions from initial surface bands can lead to intensity resonances.[18] In order to identify possible initial states for 2PPE, we have performed ARPES measurements of graphene on Ir(111). The ARPES data in Fig. 2(b) show two paraboliclike dispersions with a downward curvature. The two branches are shifted from $k_\parallel = 0$ by $\pm 0.033 \pm 0.001$ Å^{-1} and have a maximum energy of -0.19 ± 0.01 eV. For details of the fitting procedure, see Ref. 24. Similar results were also obtained with the fourth harmonic (6.2 eV) in the 2PPE setup. Rashba-type splittings of similar magnitude are found in other systems, e.g., a Bi/Ag(111) surface alloy.[25] These bands are also observed on clean Ir(111),[26,27] indicating that this surface feature is inherent to the clean metal surface. The surface-state energy reported for clean and graphene-covered surfaces differs by about 0.2 eV, an effect which is consistent with a charge

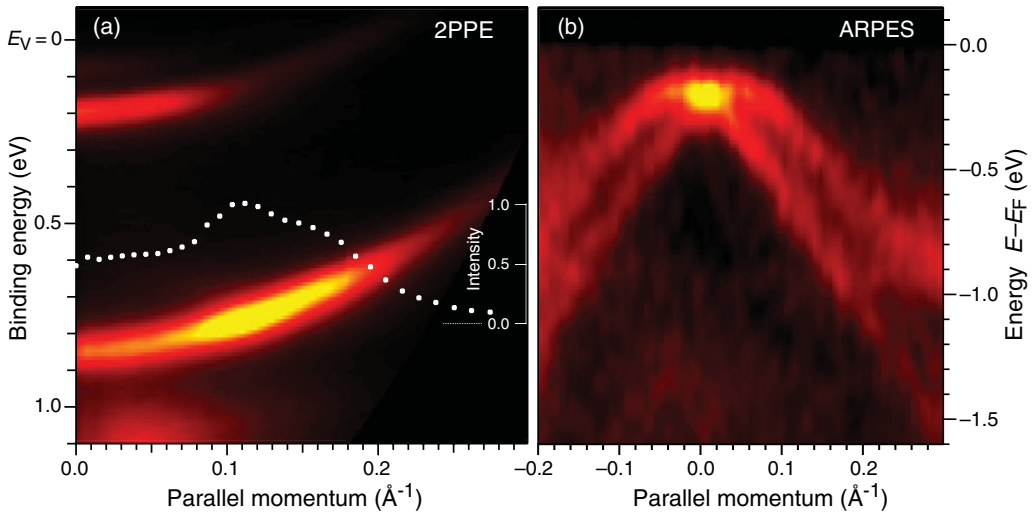

FIG. 2. (Color online) (a) Intensity map of the 2PPE signal recorded with photon energy $h\nu = 1.59$ eV for 1-ML graphene on Ir(111). Points represent the intensity of the lowest $n = 1$ band. (b) ARPES map showing initial states for $h\nu = 55$ eV.

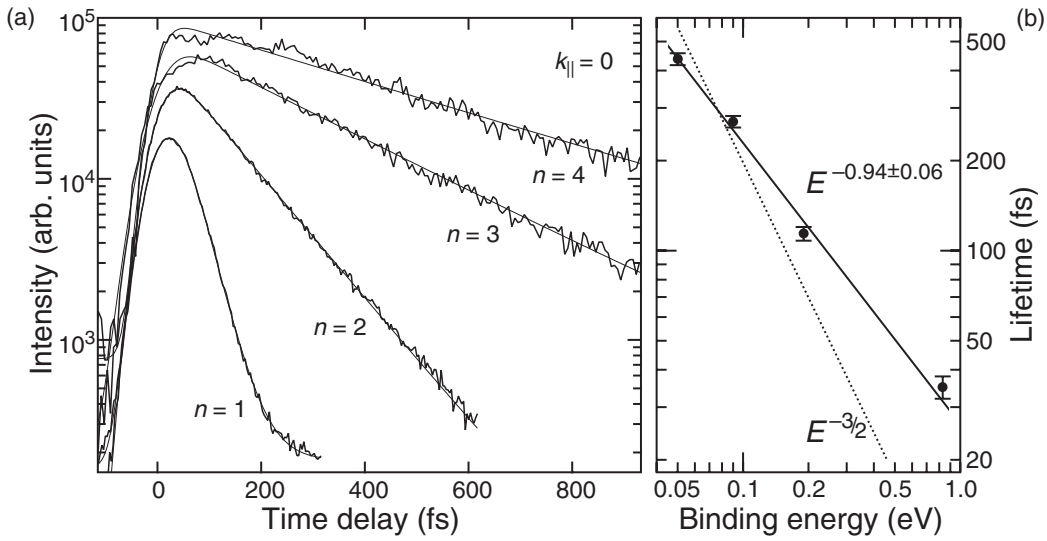

FIG. 3. (a) Time-resolved measurements of the image-potential-state series at $k_{\|} = 0$. (b) Lifetimes as a function of binding energy compared to various power-law dependencies (see text).

transfer between the substrate and overlayer and which can shift graphene[27] or iridium states.[28,29]

The initial band dispersion is plotted together with the measured dispersion of the image-potential states in Fig. 1 (blue dots). The arrows connecting initial states to the $n = 1$ image-potential band are at slightly larger $k_{\|}$ values than the enhanced intensity in Fig. 2(a). In the absence of resonances the 2PPE intensity along image-potential bands decreases continuously with increasing parallel momentum.[23] In the present case, due to the finite energy and angle resolution, the intensity maxima are shifted to lower $k_{\|}$ values compared to the position found in the dispersion analysis. The additional resonance into the $n = 2$ band (see Fig. 1) can be inferred from the similar intensity as for the $n = 1$ state at $k_{\|} = 0$ in Fig. 2(a) and is confirmed by photon-energy-dependent data taken with a display-type analyzer[30] at lower resolution.[31,32]

In order to understand the character of the initial state, we calculated the projected bulk-band structure of Ir(111) using a nonrelativistic parametrized tight-binding scheme.[33] Figure 1 shows this projected structure along the ΓK direction, at the right-hand side. The shading represents the one-dimensional density of states (1D DOS). The left-hand side of Fig. 1 shows the 1D DOS of bands according to their sp character. For $k_{\|} = 0$, the lower edge of the sp-band gap is at -0.7 eV, which corresponds to the $L_{2'}$ point. The band edge of the total projected bulk-band structure disperses upward from the L_3 point around $+0.8$ eV and picks up sp contributions. On the other hand, the lower sp-band edge shows a downward dispersion. The energy of the Shockley surface state was calculated using the sp-band edges within a scattering model.[34] The calculations used the experimental work function of 4.65 eV for graphene on Ir(111). The calculated bands were shifted by ± 0.033 Å^{-1} to account for the experimentally observed Rashba splitting and are drawn as green lines in Fig. 1 in the region below the Fermi energy. The experimentally extracted dispersion shown by dots agrees well with the calculation. The Shockley-type surface state is apparently not quenched by the graphene layer at a distance of 3.4 Å,[35] because its probability density is concentrated at the Ir(111) surface.

The scattering model was also used to calculate the energies of the image-potential-band series.[34] The calculated binding energies, given in Table I, are approximately those expected for states located near the midgap (see Fig. 1). However, the calculated $n = 1$ binding energy is significantly smaller than the experimental value. This discrepancy is due to the fact that the scattering model calculation neglects the round-trip phase shift $2\phi_{gr}$ of the graphene layer. Using the expressions for the phase shift at the substrate and the image-potential barrier,[36] we obtain $\phi_C = 0.63\pi$ and $\phi_B = 1.02\pi$, respectively. The total phase shift for the $n = 1$ state is 2π, from which we obtain $\phi_{gr} = 0.18\pi$. Note that such a small phase shift leads to a significant change in binding energy from 0.59 to 0.83 eV (see Table I).

The time-resolved spectra of the image-potential states were also measured and are shown in Fig. 3(a). As summarized in Table I, lifetimes of tens to hundreds of femtoseconds are obtained. These are comparable to values obtained for Cu(100) with a similar midgap image-potential-state position and hence bulk evanescent decay length in the metal crystal.[21] Note, as an aside, that the curve measured at the energy of the $n = 4$ image-potential state in Fig. 3(a) shows weak quantum beats[21] for delay times <300 fs. The data in Table I show that lifetimes vary with the binding energy approximately $\propto E^{-1}$ [solid line in Fig. 3(b)]. The asymptotic, classical $\tau \propto E^{-3/2}$ behavior[37] [dashed line in Fig. 3(b)] is not reached for $n < 4$. Similar behavior has been found on copper surfaces.[38]

An important issue for carrier movement at graphene/metal interfaces is the degree of lateral confinement. This confinement can be examined at low graphene coverage, obtained via a small number of sequential TPG cycles. From previous studies, it is known that one TPG cycle covers a fraction of about 20% of the uncovered Ir surface.[28] After one TPG cycle the typical island size is $(35\ \text{nm})^2$ and after the second cycle of the order of $(100\ \text{nm})^2$.[28]

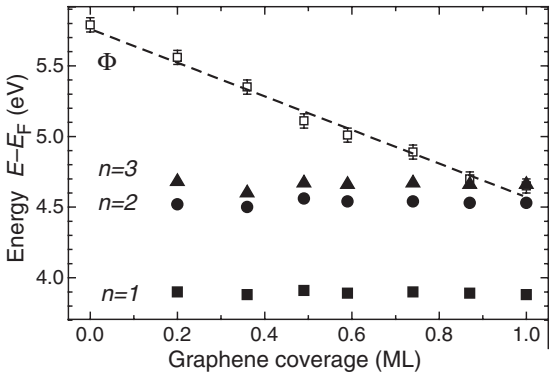

FIG. 4. Sample work function (open symbols) and image-potential states $n = 1$, 2, and 3 binding energies (solid symbols) as a function of graphene coverage. The dashed line represents a linear fit for the work-function change.

As has been shown in earlier work[39] that the average and local work functions play an important role in interfacial electron localization. Thus the average work function Φ was measured via monochromatic 2PPE and the expression $\Phi = 2h\nu - \Delta E$, i.e., where $h\nu$ is the photon energy and ΔE is the difference between the Fermi level cutoff and the low-energy cutoff. Figure 4 displays the work function (open symbols) as a function of graphene coverage. The work function decreases approximately linearly from a value 5.79 ± 0.10 to 4.65 ± 0.10 eV from Ir(111) to 1-ML graphene. Reported values of the work function for Ir(111) are 5.76 and 5.79 eV.[40] The work function of the graphene-covered surface on Ir(111) is between the values for Pt(111) of 4.87 eV and free-standing graphene of 4.48 eV,[41] which is consistent with the weak bonding between the Ir(111) and the graphene overlayer and a *p* doping of the graphene.[12] The linear decrease of the work function is known for other systems and is due to the averaging over substrate and overlayer islands.[39]

Image-potential states were observed at all coverages reported here using 2PPE. However, for the clean surface or uncovered substrate areas the available photon energies were not sufficient to populate image-potential states due to the large work function of Ir(111); thus no image-potential states were seen in the absence of any graphene coverage. The image-potential-state energies, measured relative to the Fermi level, are shown in Fig. 4. The energies are generally constant over the coverage range from 0.2 to 1 ML, with the intensity increasing monotonically with coverage. Note that the graphene Dirac cone at the *K* point has been clearly observed for more than three TPG cycles or 0.5-ML graphene coverage.[28] The constant energy of the image-potential series as a function of coverage in Fig. 4 is a direct result of the localization of the electrons on the graphene islands.[39] The electrons respond to the local work function if the average island dimensions are larger than the typical distance of the probability density maximum, which is of the order of nanometers for the lowest *n* image-potential states. Note that the localization on the graphene islands is facilitated by the large work-function difference between the graphene layers and the Ir(111) substrate. For small graphene islands, an energy shift proportional to d^{-2}, where d denotes the characteristic island size, is expected due to the lateral localization of the electron in a two-dimensional quantum well.[42] However, these shifts would be <1 meV for the island sizes expected for the current preparation conditions.[28]

In summary, we have observed and measured the properties of image-potential states on a graphene monolayer on Ir(111). The binding energy of the $n = 1$ image-potential state is 40% larger than expected from the position of the graphene vacuum level relative to the Ir(111) band gap. There is no prominent indication of a second main series of image-potential states as predicted for free-standing graphene.[11] Apparently, the underlying metal substrate breaks the mirror symmetry of the graphene layer and the state of odd symmetry shifts up in energy, as has been calculated for graphene on Ru(0001).[17] In addition, the image-potential states can be excited efficiently from a downward dispersing Shockley surface state in the *sp*-band gap of the Ir(111) band structure, indicating a sizable overlap of the wave functions of these states located at the substrate interface and graphene surface, respectively. The measured lifetimes of the image-potential states are comparable to similar clean metal surfaces. Recently, similar results have also been obtained for graphene on Pt(111).[43] Apparently, the evanescent coupling of the image-potential-state wave functions to the underlying electronic states of the Ir(111) bulk and surface states is not altered by the graphene layer. Three-dimensional localization of electrons on graphene islands has been observed for submonolayer coverages obtained by individual TPG cycles. However, even for the smallest island size, no energy shift due to localization was observed within the experimental uncertainty. Further development is needed to prepare well-ordered graphene islands with controlled lateral extension. A different approach would be to exploit the moiré pattern on more corrugated graphene layers.[10,17]

We acknowledge helpful discussions with Pedro Echenique and Branko Gumhalter. The work at Columbia University was financially supported by the US Department of Energy under Contract No. DE-FG 02-04-ER-46157. The Zagreb group acknowledges funding by the MZOS through Project No. 035-0352828-2840 and by MZOS-NSF through Contract No. 1/2009. M.K. thanks the AvH Foundation for financial support.

[1] A. H. Castro Neto, F. Guinea, N. M. R. Peres, K. S. Novoselov, and A. K. Geim, Rev. Mod. Phys. **81**, 109 (2009).

[2] X. Li, W. Cai, J. An, S. Kim, J. Nah, D. Yang, R. Piner, A. Velamakanni, I. Jung, E. Tutuc, S. K. Banerjee, L. Colombo, and R. S. Ruoff, Science **324**, 1312 (2009).

[3] J. Coraux, A. T. N'Diaye, C. Busse, and T. Michely, Nano Lett. **8**, 565 (2008).

[4] P. W. Sutter, J. I. Flege, and E. A. Sutter, Nat. Mater. **7**, 406 (2008).

[5] I. Meric, C. R. Dean, A. F. Young, N. Baklitskaya, N. J. Tremblay, C. Nuckolls, P. Kim, and K. L. Shepard, Nano Lett. **11**, 1093 (2011).

[6]Y. Zhang, Y. W. Tan, H. L. Stormer, and P. Kim, Nature (London) **438**, 201 (2005).
[7]T. Ohta, A. Bostwick, T. Seyller, K. Horn, and E. Rotenberg, Science **313**, 951 (2006).
[8]A. Bostwick, T. Ohta, T. Seyller, K. Horn, and E. Rotenberg, Nat. Phys. **3**, 36 (2006).
[9]K. R. Knox, A. Locatelli, M. B. Yilmaz, D. Cvetko, T. O. Menteş, M. Á. Niño, P. Kim, A. Morgante, and R. M. Osgood Jr., Phys. Rev. B **84**, 115401 (2011).
[10]N. Armbrust, J. Güdde, P. Jakob, and U. Höfer, Phys. Rev. Lett. **108**, 056801 (2012).
[11]V. M. Silkin, J. Zhao, F. Guinea, E. V. Chulkov, P. M. Echenique, and H. Petek, Phys. Rev. B **80**, 121408 (2009).
[12]I. Pletikosić, M. Kralj, P. Pervan, R. Brako, J. Coraux, A. T. N'Diaye, C. Busse, and T. Michely, Phys. Rev. Lett. **102**, 056808 (2009).
[13]Z. Sun, S. K. Hämäläinen, J. Sainio, J. Lahtinen, D. Vanmaekelbergh, and P. Liljeroth, Phys. Rev. B **83**, 081415 (2011).
[14]R. van Gastel, A. T. N'Diaye, D. Wall, J. Coraux, C. Busse, N. M. Buckanie, F.-J. M. zu Heringdorf, M. H. von Hoegen, T. Michely, and B. Poelsema, Appl. Phys. Lett. **95**, 121901 (2009).
[15]F. Xia, V. Perebeinos, Y. Lin, Y. Wu, and P. Avouris, Nat. Nanotechnol. **6**, 179 (2011).
[16]S. Bose, V. M. Silkin, R. Ohmann, I. Brihuega, L. Vitali, C. H. Michaelis, P. Mallet, J. Y. Veuillen, M. A. Schneider, E. V. Chulkov, P. M. Echenique, and K. Kern, New J. Phys. **12**, 023028 (2010).
[17]B. Borca, S. Barja, M. Garnica, D. Sánchez-Portal, V. M. Silkin, E. V. Chulkov, C. F. Hermanns, J. J. Hinarejos, A. L. Vázquez de Parga, A. Arnau, P. M. Echenique, and R. Miranda, Phys. Rev. Lett. **105**, 036804 (2010).
[18]Z. Hao, J. I. Dadap, K. R. Knox, M. B. Yilmaz, N. Zaki, P. D. Johnson, and R. M. Osgood, Phys. Rev. Lett. **105**, 017602 (2010).
[19]K. Boger, Th. Fauster, and M. Weinelt, New J. Phys. **7**, 110 (2005).
[20]H. Hattab, A. T. N'Diaye, D. Wall, G. Jnawali, J. Coraux, C. Busse, R. van Gastel, B. Poelsema, T. Michely, F.-J. M. zu Heringdorf, and M. H. von Hoegen, Appl. Phys. Lett. **98**, 141903 (2011).
[21]U. Höfer, I. L. Shumay, Ch. Reuß, U. Thomann, W. Wallauer, and Th. Fauster, Science **277**, 1480 (1997).
[22]P. M. Echenique and J. B. Pendry, J. Phys. C **11**, 2065 (1978).
[23]J. Güdde, M. Rohleder, T. Meier, S. W. Koch, and U. Höfer, Science **318**, 1287 (2007).
[24]See Supplemental Material at http://link.aps.org/supplemental/10.1103/PhysRevB.85.081402 for details of the fitting of the ARPES spectra.
[25]C. R. Ast, J. Henk, A. Ernst, L. Moreschini, M. C. Falub, D. Pacilé, P. Bruno, K. Kern, and M. Grioni, Phys. Rev. Lett. **98**, 186807 (2007).
[26]J. F. van der Veen, F. J. Himpsel, and D. E. Eastman, Phys. Rev. B **22**, 4226 (1980).
[27]I. Pletikosić, M. Kralj, D. Sokcević, R. Brako, P. Lazić, and P. Pervan, J. Phys. Condens. Matter **22**, 135006 (2010).
[28]M. Kralj, I. Pletikosić, M. Petrović, P. Pervan, M. Milun, A. T. N'Diaye, C. Busse, T. Michely, J. Fujii, and I. Vobornik, Phys. Rev. B **84**, 075427 (2011).
[29]D. Subramaniam, F. Libisch, Y. Li, C. Pauly, V. Geringer, R. Reiter, T. Mashoff, M. Liebmann, J. Burgdörfer, C. Busse, T. Michely, R. Mazzarello, M. Pratzer, and M. Morgenstern, Phys. Rev. Lett. **108**, 046801 (2012).
[30]D. Rieger, R. D. Schnell, W. Steinmann, and V. Saile, Nucl. Instrum. Methods **208**, 777 (1983).
[31]R. Matzdorf, Surf. Sci. Rep. **30**, 153 (1998).
[32]See Ref. 24 for data showing the resonant transition into the $n = 2$ state.
[33]D. A. Papaconstantopoulos, *Handbook of the Band Structure of Elemental Solids* (Plenum, New York, 1986).
[34] Th. Fauster, Appl. Phys. A **59**, 639 (1994).
[35]C. Busse, P. Lazić, R. Djemour, J. Coraux, T. Gerber, N. Atodiresei, V. Caciuc, R. Brako, A. T. N'Diaye, S. Blügel, J. Zegenhagen, and T. Michely, Phys. Rev. Lett. **107**, 036101 (2011).
[36]N. V. Smith, Phys. Rev. B **32**, 3549 (1985).
[37] Th. Fauster, Ch. Reuß, I. L. Shumay, and M. Weinelt, Chem. Phys. **251**, 111 (2000).
[38]P. M. Echenique, R. Berndt, E. V. Chulkov, Th. Fauster, A. Goldmann, and U. Höfer, Surf. Sci. Rep. **52**, 219 (2004).
[39]R. Fischer, S. Schuppler, N. Fischer, Th. Fauster, and W. Steinmann, Phys. Rev. Lett. **70**, 654 (1993); R. Fischer, Ph.D. thesis, Universität München, 1993.
[40]R. W. Strayer, W. Mackie, and L. W. Swanson, Surf. Sci. **34**, 225 (1973);. B. E. Nieuwenhuys, R. Bouwman, and W. M. H. Sachtler, Thin Solid Films **21**, 51 (1974).
[41]G. Giovannetti, P. A. Khomyakov, G. Brocks, V. M. Karpan, J. van den Brink, and P. J. Kelly, Phys. Rev. Lett. **101**, 026803 (2008).
[42]R. Fischer, Th. Fauster, and W. Steinmann, Phys. Rev. B **48**, 15496 (1993).
[43]D. Nobis, D. Niesner, and Th. Fauster (unpublished).